Ceramics International 47 (2021) 29888–29899

Contents lists available at ScienceDirect

Ceramics International

journal homepage: www.elsevier.com/locate/ceramint

Ceramic pigments from $Co_xNi_{3-x}P_2O_8$ ($0 \leq x \leq 3$) solid solutions

M.A. Tena [a,*], Rafael Mendoza [b], Camino Trobajo [c], José R. García [c], Santiago García-Granda [d]

[a] Inorganic Chemistry Area. Inorganic and Organic Chemistry Department. Jaume I University, P.O. Box 224, Castellón, Spain
[b] Physical Chemistry Area. Scientific and Technical Services. Oviedo University-CINN, Spain
[c] Inorganic Chemistry Area. Organic and Inorganic Chemistry Department. Oviedo University-CINN, Spain
[d] Physical Chemistry Area. Physical and Analytical Chemistry Department. Oviedo University-CINN, Spain

ARTICLE INFO

Keywords:
$Ni_3P_2O_8$
$Co_3P_2O_8$
Solid solutions
Ceramic pigments

ABSTRACT

$Co_xNi_{3-x}P_2O_8$ ($0 \leq x \leq 3$) solid solutions were synthesized via the chemical co-precipitation method. Variation of unit cell parameters and interatomic distances indicated that these solid solutions with the $Ni_3P_2O_8$ structure are stable between 800 and 1200 °C in compositions with $0 \leq x \leq 1.5$ and between 800 and 1000 °C when ($0 \leq x \leq 3$). When ($2.5 \leq x \leq 3.0$), the solid solutions lead to the $Co_3P_2O_8$ structure, being stable between 800 and 1000 °C.

The yellow colour of the $Ni_3P_2O_8$ compound changes to pink or red when Co(II) ions are incorporated in the structure as $Ni_3P_2O_8$ solid solutions are formed. Bands corresponding to second and third electronic transitions of the Co(II) ions in octahedral coordination appear in the 450–600 nm in the UV-V spectra, and they are responsible of the observed changes in the colour. Absorbance in the visible spectra was also obtained from enamelled samples but a new band at 650 nm with considerable absorbance when $x > 1.0$ increased the blue amount, and colour of the enamelled samples was yellowish brown, brown, green and blue.

1. Introduction

Metal phosphate structures are chemically very stable. These structures show fast charge transport by reducing the diffusion path length through the structure [1]. Phosphate pigments exhibit a partial chemical, thermal stability and resistivity to dissolution agents, hence allowing their use as an efficient colouring agent for the colouration of ceramic glazes [2]. The strong P − O covalent bonds allow the strong charge transfer in M − O bonds when M = Co (blue or purple), Ni (yellow) and Cu (bluish green) [3–5].

$Co_{2-x}Ni_xP_2O_7$ ($0 \leq x \leq 2$) solid solutions with an α-$M_2P_2O_7$ structure fired between 800 and 1200 °C show blue ($x = 0$), green ($0 < x < 2$) and yellow ($x = 2$) colours. These materials avoid the pinhole defect due to the presence of Co_3O_4 formed when CoO and cobalt salts are used as raw materials in the synthesis of ceramic pigments [3]. The M(II) is in octahedral and a square planar pyramid coordination in α-$M_2P_2O_7$ structure and the sum of the Co(II) and Ni(II) spectra in the two different crystallographic sites can be detected from green solid solutions.

The Ni(II) ion is only in octahedral coordination in the lemon yellow $Ni_3P_2O_8$ compound [6], and Ni(II) is in both octahedral and square planar pyramid coordination in the bright yellow α-$Ni_2P_2O_7$ compound. These compounds can be used as ceramic pigments due to its thermal and chemical stability into commercial glazes [4]. Colour modification is expected from solid solutions with the α-$Ni_2P_2O_7$ or $Ni_3P_2O_8$ structure. Only a polymorph of the $Ni_3P_2O_8$ compound with $Fe_3(PO_4)_2$ type monoclinic structure is described in the bibliography (ICSD-153160) [6,7] while two structures have been reported from the $Co_3P_2O_8$ compound. The olivine-related polymorph of the $Co_3P_2O_8$ compound (ICSD-9850) [7,8] is isostructural with $Ni_3P_2O_8$ compound, and all the Co(II) ions are in octahedral coordination in it. The transition temperature from olivine-related to stable phase is 870 °C [8]. The stable polymorph of $Co_3P_2O_8$ compound, with $Mg_3P_2O_8$ monoclinic structure, contains Co(II) in both octahedral and square planar pyramid coordination (ICSD-38259) [9]. Fig. 1 shows the $Ni_3P_2O_8$ and the stable $Co_3P_2O_8$ structures from ICSD-153160 and ICSD-38259 data [6,7,9]. The structure was drawn with the Studio program [10–12], and three polyhedra have been highlighted in the structure. The central octahedron in these groups is attached to the other polyhedra sharing 2 oxygens with each one. Two octahedral different crystallographic sites M1 (2a special site) and M2 (4e general site) are present in the $Ni_3P_2O_8$ structure and therefore in compounds, polymorphs or solid solutions with this structure. In the stable $Co_3P_2O_8$ structure, the CoO_6 octahedra

* Corresponding author.
E-mail addresses: tena@qio.uji.es (M.A. Tena), mendozarafael@uniovi.es (R. Mendoza), ctf@uniovi.es (C. Trobajo), jrgm@uniovi.e (J.R. García), s.garciagranda@cinn.es (S. García-Granda).

https://doi.org/10.1016/j.ceramint.2021.07.162
Received 7 April 2021; Received in revised form 11 June 2021; Accepted 16 July 2021
Available online 17 July 2021

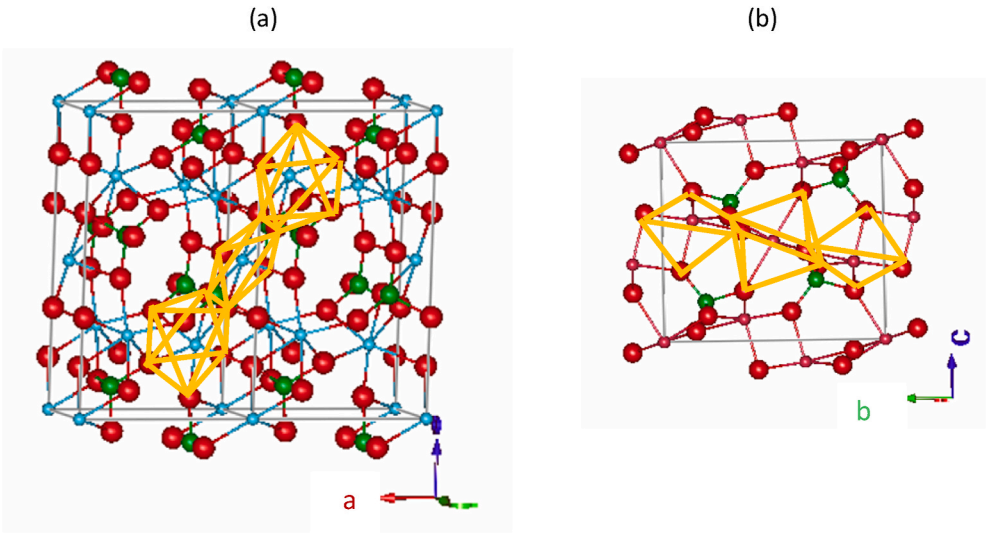

Fig. 1. $Ni_3P_2O_8$ (a) and the stable $Co_3P_2O_8$ (b) structures from ICSD-153160 and ICSD-38259 data.

Table 1
Evolution of crystalline phases with temperature in $Co_xNi_{3-x}P_2O_8$ ($0.0 \leq x \leq 3.0$) compositions.

X	600 °C	800 °C	1000 °C	1200 °C
0.0	–	A(s), B(vw)	A(s)	A(s)
0.5	–	A(s)	A(s)	A(s)
1.0	C (vw)	A(s)	A(s)	A(s)
1.5	C(w), D(vw)	A(s)	A(s)	A(s), D(vw)
2.0	C(w), D(w)	A(s), D(w)	A(s)	A(m), D(m)
2.5	D(m)	D(s), A(w)	D(s)	–
3.0	D(m)	D(s)	D(s)	–

Crystalline phases: A = $M_3P_2O_8$ solid solutions (M = Co, Ni) with $Ni_3P_2O_8$ structure (Ni(II), CN = 6).
B = $Ni_3P_2O_8$ (Ni(II), CN = 5, 6), C = olivine-related $Co_3P_2O_8$ (Co(II), CN = 6).
D = stable $Co_3P_2O_8$ (Co(II), CN = 5, 6).
Diffraction peak intensity: s = strong, m = medium, w = weak, vw = very weak.

share two opposite edges of a plane, each with a square-based pyramid CoO_5 and the oxygens at the other 2 vertices of the octahedron are each joined to another CoO_5 pyramid. In addition, each CoO_6 octahedron is linked to four PO_4 tetrahedra.

Structural information about $Co_xNi_{3-x}P_2O_8$ solid solutions with the $Ni_3P_2O_8$ structure can be found in ICSD-30800 and ICSD-30801 [7,13], but information about the $Co_xNi_{3-x}P_2O_8$ solid solutions at $T \geq 1000$ °C has not been published. At $T > 870$ °C, solid solutions with the $Co_3P_2O_8$ stable structure might be obtained in cobalt-rich compositions.

In $M_xNi_{3-x}(PO_4)_2$ (M = Mg, Mn, Fe, Co, Cu, or Zn) solid solutions with the $Ni_3P_2O_8$ structure, prepared from metal oxides and $NH_4H_2PO_4$ at 1200 K (927 °C) and equilibrated at 1070 K (797 °C), the octahedra around M2 are slightly larger than the octahedra around M1. So, M2-O distances are larger than M1-O distances. The difference in average M2-O and M1-O distances are approximately 0.002 Å (ICSD-153160) when M = Ni and approximately 0.228 Å when M = Co (ICSD-9850). The Ni^{2+}/M distributions are mainly controlled by crystal field energies, while the size effects are small. The preference for M1 over M2 is $Ni^{2+} > Co^{2+} > Mg^{2+}$, $Zn^{2+} > Mn^{2+} >> Fe^{2+}$ [13]. The synthesis via hydrothermal with pyrolysis at low temperature of $Co_xNi_{3-x}(PO_4)_2$ compositions [14] develops amorphous materials after pyrolysis, when the temperature is lower than 400 °C. The crystalline phase with the olivine-related $Co_3(PO_4)_2$ structure is developed between 500 and 700 °C. These solid solutions are stable at 800 °C [14]. Stability at $T > 800$ °C is not reported. Unit cell parameters in $Co_{1.5}Ni_{1.5}P_2O_8$ composition are between the $Ni_3P_2O_8$ and the olivine-related $Co_3P_2O_8$ unit cell parameters [15]. The mesoporous shell-like $Co_{3-x}Ni_x(PO_4)_2$ hollow structures synthesized via one-pot oil-in-water emulsion method with large specific surface area at 185 °C has potential applications in biosensors, energy storage and electrocatalysis [16].

The aim of this study is to synthesize $Co_xNi_{3-x}P_2O_8$ ($0 \leq x \leq 3$) solid solutions, to check their stability at temperature higher than 900 °C, to follow the evolution of their colour with temperature and to compare the colorations of the solid solutions with orthophosphate and diphosphate structures.

2. Experimental

$Co_xNi_{3-x}P_2O_8$ ($0 \leq x \leq 3$) compositions were synthesized from $Co(NO_3)_2{\cdot}6H2O$ (Acros Organic, 99%), $Ni(NO_3)_2{\cdot}6H2O$ (Acros Organic, 99%) and H_3PO_4 (Merck, 99%) via the chemical co-precipitation method.

The stoichiometric amount of $Co(NO_3)_2{\cdot}6H_2O$, $Ni(NO_3)_2{\cdot}6H_2O$ and a 0.5 M solution of H_3PO_4 in water were added to water to obtain a final volume of 200 mL. Samples were vigorously stirred for 22 h at room temperature. Then, an ammonia aqueous solution (Panreac, 25%) was added with continuous stirring until reaching pH = 10. In these conditions, the materials were co-precipitated. The obtained materials were dried in a stove at 65 °C to evacuate only the water. The Co:Ni:P molar ratio of the starting materials was preserved in this process. The dry samples were fired at 300, 600, 800, 1000 and 1200 °C for 6 h at each temperature.

The development of the crystalline phases at different temperatures was studied by XRD. The resulting materials were examined using a Panalytical X-ray diffractometer (Malvern Panalytical, Almelo, The Netherlands) with CuK_α radiation. The unit cell parameters and interatomic distances in the developed structures were determined to investigate the possible formation of solid solutions under these synthesis conditions. A structure profile refinement was carried out via the Rietveld method (Fullprof.2 k computer program) [10–12]. Diffraction patterns ranging between 6 and 110° (2θ) were collected employing monochromatic CuK_α radiation, a step size of 0.02° (2θ) and a sampling time of 10 s. The initial structural information was taken from the Inorganic Crystal Structure Database [7]. This database includes standard cell, standard space group, fractional atomic coordinates and other information on crystalline phases found in the literature.

The Co(II) and Ni(II) sites and the transfer charge bands in the samples were studied by UV–vis–NIR spectroscopy (diffuse reflectance). The ultraviolet visible near infrared (UV–vis–NIR) spectra in the 200–2500 nm range were obtained using a Jasco V-670 spectrophotometer. To test their efficiency as ceramic pigments, the compositions

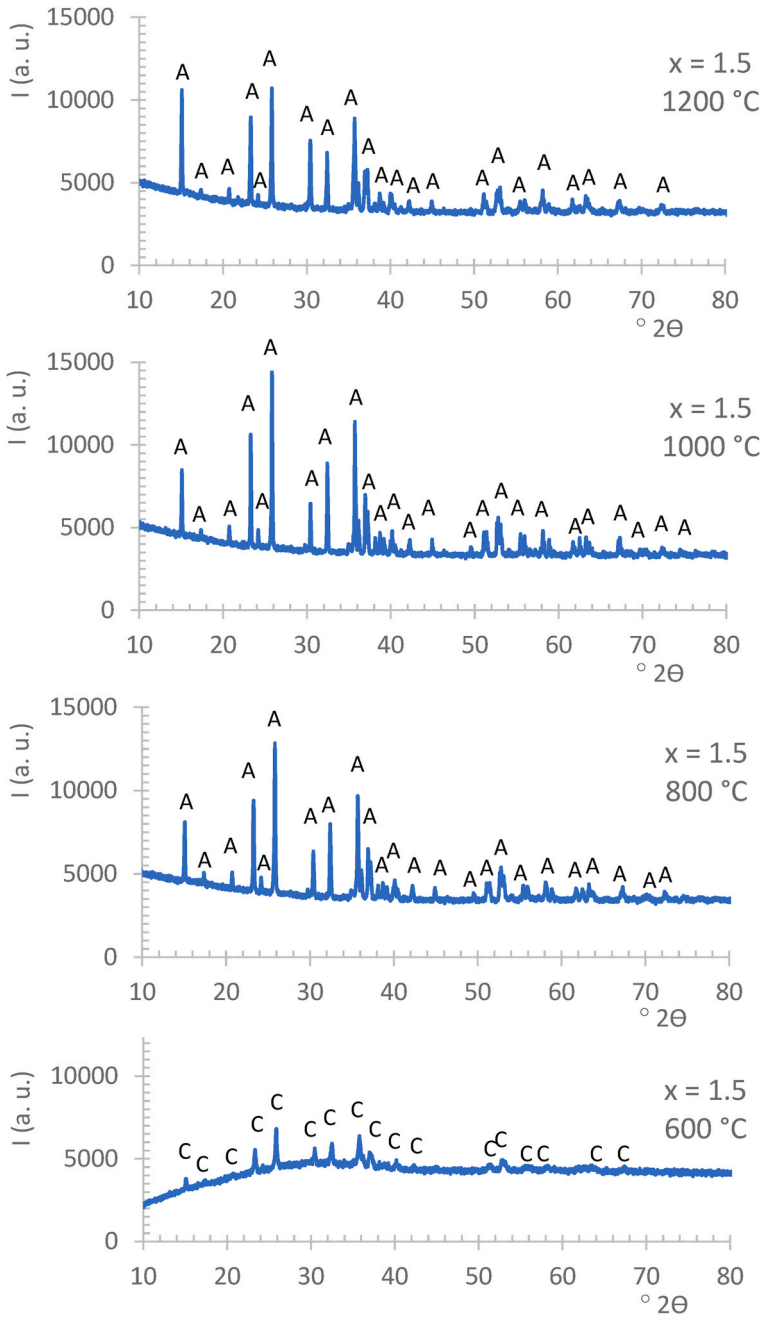

Crystalline phases: C = olivine-related $Co_3P_2O_8$, A = $M_3P_2O_8$ solid solutions (M = Co, Ni) with $Ni_3P_2O_8$ structure

Fig. 2. Evolution of the crystalline phases with temperature from $Co_{1.5}Ni_{1.5}P_2O_8$ composition.

fired at 1000 °C were 4% weight enamelled with a commercial glaze (SiO_2 – Al_2O_3 – PbO – Na_2O – CaO glaze) onto commercial ceramic biscuits. Many pigments are dissolved in this glaze. The colour of the material is lost when this occurs. Glazed tiles were fired for 15 min at 1065 °C, subsequently obtained their UV–vis–NIR spectra.

The CIEL*a*b* colour parameters on the fired samples: L* is the lightness axis (black (0) → white (100)), a* is the green (-) → red (+) axis, and b* is the blue (-) → yellow (+) axis [17] were obtained with an X-Rite spectrophotometer (SP60, standard illuminant D65, an observer 10°, and a reference sample of MgO). The measurements were performed on powdered samples and on glazed tiles.

3. Results and discussion

Table 1 shows the evolution of the crystalline phases with composition and temperature in $Co_xNi_{3-x}P_2O_8$ ($0.0 \leq x \leq 3.0$) compositions. This evolution from composition with $x = 1.5$ ($Co_{1.5}Ni_{1.5}P_2O_8$) is shown in Fig. 2. At 600 °C, $Ni_3P_2O_8$ composition is not a crystalline material in the conditions of this study. A poorly crystalline phase with the $Ni_3P_2O_8$ structure (or olivine-related $Co_3P_2O_8$ structure) is detected when $1.0 \leq x \leq 2.0$ and a developed crystalline phase with the stable $Co_3P_2O_8$ structure when $x \geq 1.5$. At 800 °C, the crystalline phase with the $Ni_3P_2O_8$ structure is detected when $0.0 \leq x \leq 2.0$ as the majority phase (>87%) and when $x = 2.5$ as the minority phase (5%). The crystalline phase with the stable $Co_3P_2O_8$ structure is detected when $x \geq 2.0$ at 800 °C (13% when $x = 2.0$, 94% when $x = 2.5$, and 100% when $x = 3.0$). At 1000 °C,

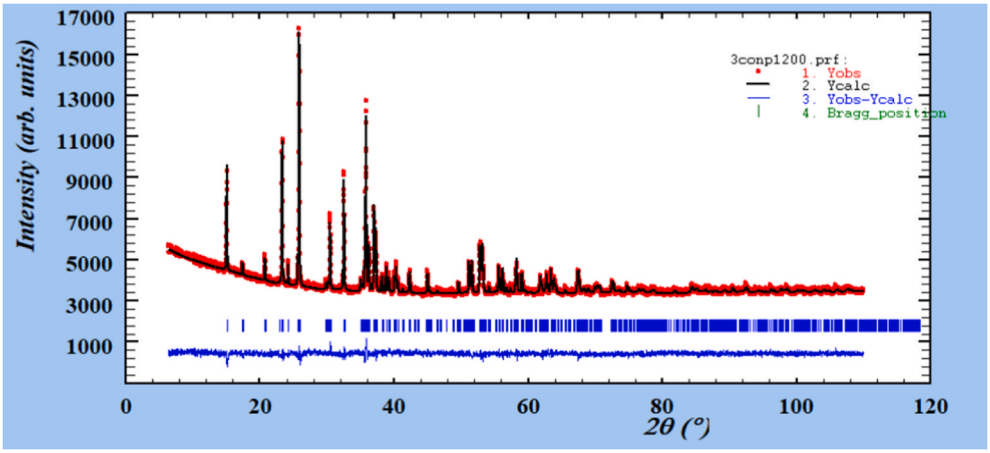

Fig. 3. The diffraction profile refinement by Rietveld's method from $CoNi_2P_2O_8$ composition fired at 1200 °C.

Table 2
Variation in unit cell parameters and volume in the $Ni_3P_2O_8$ (or olivine-related $Co_3P_2O_8$) and stable $Co_3P_2O_8$ structures obtained from $Co_xNi_{3-x}P_2O_8$ ($0.0 \leq x \leq 3.0$) compositions.

x	Structure		800 °C	1000 °C	1200 °C
0.0	$Ni_3P_2O_8$	a (Å)	5.82653(5)	5.82635(5)	5.82652(5)
		b (Å)	4.69627(5)	4.69600(4)	4.69483(4)
		c (Å)	10.10524(9)	10.10520(8)	10.10312(8)
		β (°)	91.1261(6)	91.1338(5)	91.1264(5)
		V (Å^3)	276.456(5)	276.429(4)	276.312(4)
0.5	$Ni_3P_2O_8$	a (Å)	5.84320(6)	5.84324(5)	5.84407(6)
		b (Å)	4.70217(5)	4.70237(4)	4.70088(5)
		c (Å)	10.1384(1)	10.13865(8)	10.13490(9)
		β (°)	91.1086(6)	91.1121(5)	91.0926(6)
		V (Å^3)	278.509(5)	278.528(4)	278.378(5)
1.0	$Ni_3P_2O_8$	a (Å)	5.8597(1)	5.85981(7)	5.86315(6)
		b (Å)	4.70912(8)	4.70903(6)	4.70850(5)
		c (Å)	10.1719(1)	10.1727(1)	10.1703(1)
		β (°)	91.0794(9)	91.0904(6)	91.0608(6)
		V (Å^3)	280.635(8)	280.656(5)	280.721(5)
1.5	$Ni_3P_2O_8$	a (Å)	5.8741(1)	5.87519(6)	5.86767(9)
		b (Å)	4.71617(9)	4.71612(6)	4.7146(1)
		c (Å)	10.2078(2)	10.2077(1)	10.1963(1)
		β (°)	91.081(1)	91.0755(7)	91.091(1)
		V (Å^3)	282.737(9)	282.787(5)	282.017(9)
2.0	$Ni_3P_2O_8$	a (Å)	5.8873(1)	5.8892(1)	5.8893(2)
		b (Å)	4.72397(9)	4.7246(1)	4.7250(1)
		c (Å)	10.2441(2)	10.2441(2)	10.2460(3)
		β (°)	91.075(1)	91.069(1)	91.061(2)
		V (Å^3)	284.856(9)	284.98(1)	285.07(1)
2.0	$Co_3P_2O_8$	a (Å)	–	–	5.0686(2)
		b (Å)	–	–	8.3111(3)
		c (Å)	–	–	8.7928(3)
		β (°)	–	–	121.387(2)
		V (Å^3)	–	–	316.20(3)
2.5	$Co_3P_2O_8$	a (Å)	5.0690(1)	5.0690(1)	–
		b (Å)	8.3132(2)	8.3132(2)	–
		c (Å)	8.7939(2)	8.7939(2)	–
		β (°)	121.259(1)	121.259(1)	–
		V (Å^3)	316.79(1)	316.79(1)	–
3.0	$Co_3P_2O_8$	a (Å)	5.0630(2)	5.0628(1)	–
		b (Å)	8.3620(2)	8.3650(2)	–
		c (Å)	8.7889(3)	8.7904(2)	–
		β (°)	121.002(1)	120.990(1)	–
		V (Å^3)	318.94(2)	319.13(1)	–

only one crystalline phase can be detected in each sample with the $Ni_3P_2O_8$ structure when $0.0 \leq x \leq 2.0$ and with the stable $Co_3P_2O_8$ structure when $x \geq 2.5$. At 1200 °C, crystalline $Ni_3P_2O_8$ phase is detected in compositions with $0.0 \leq x \leq 2.0$ although this crystalline phase appears together to the crystalline stable $Co_3P_2O_8$ phase when $1.5 \leq x \leq 2.0$. At this temperature, in these compositions the partial transition from olivine-related $Co_3P_2O_8$ phase ($Ni_3P_2O_8$ structure) to stable $Co_3P_2O_8$ phase occurs. Compositions with $x \geq 2.0$ melted at 1200 °C and the higher cobalt compositions ($x \geq 2.0$) could not be removed from the crucible.

Fig. 3 shows graphical result of the diffraction profile refinement by Rietveld's method from $CoNi_2P_2O_8$ composition ($x = 1.0$) fired at 1200 °C. Table 2 includes the unit cell parameters and volume in $Ni_3P_2O_8$ and stable $Co_3P_2O_8$ structures from $Co_xNi_{3-x}P_2O_8$ ($0.0 \leq x \leq 3.0$) compositions fired at 800, 1000 and 1200 °C. Increasing the unit cell parameters with x is consistent with the replacement of the Ni(II) ion by the larger Co(II) ion. The crystalline phase with $Ni_3P_2O_8$ structure is detected with increasing cell parameters when $0.0 \leq x \leq 2.0$ both in this study and in the bibliography [13] at 800 °C. Fig. 4 compares the unit cell parameters in $Ni_3P_2O_8$ structure in the prepared compositions in this study and the values in the literature [13] at 800 °C. Values are similar and the limit of formation of these solid solutions is $x = 2.0$ at this temperature. At 800, 1000 and 1200 °C similar values of unit cell parameters were obtained in $Ni_3P_2O_8$ structure ($0.0 \leq x \leq 2.0$) and at 800–1000 °C in the stable $Co_3P_2O_8$ structure ($2.5 \leq x \leq 3.0$). The formation limit of these solid solutions with $Ni_3P_2O_8$ structure is also $x = 2.0$ at 1000 °C. The variation of the unit cell parameters with x is practically lineal according to the Vegard's law (Fig. 5). Thus, in the $Co_xNi_{3-x}P_2O_8$ solid solutions with the $Ni_3P_2O_8$ structure ($0.0 \leq x \leq 2.0$), the Ni(II) and Co(II) ions are practically randomly distributed at 800 and 1000 °C. A slight departure of Vegard's law is detected in the variation of the unit cell parameters with composition (with x). The changes in unit cell parameters with composition are not governed purely by the relative sizes of the Co(II) and Ni(II) ions.

A slight increase in M − O distances (M = Co, Ni) with x is detected from $Co_xNi_{3-x}P_2O_8$ ($0.0 \leq x \leq 2.0$) solid solutions with the $Ni_3P_2O_8$ structure at $800 \leq T \leq 1200$ °C (Table 3). All of M1-O distances are approximately 2.09 Å. The longest and smallest M2-O distances are approximately 2.19 Å and 2.01 Å, respectively. So, octahedra around M2 are more distorted than octahedra around M1. No significant changes with x are detected in P–O distances. Fig. 6 shows the variation of the M − O and P–O distances with the composition at 1000 °C. The slight increase in the M − O distances with x is in accordance with the incorporation of the Co(II) ion to the structure with a larger radius than the Ni (II) ionic radius. No significant distortions are detected in these solid solutions. Three similar values and one higher value of P–O distances is obtained in all of the $Co_xNi_{3-x}P_2O_8$ ($0.0 \leq x \leq 2.0$) compositions with the $Ni_3P_2O_8$ structure (Table 4 and Fig. 6).

Fig. 7 shows the UV–vis–NIR spectra of the $Ni_3P_2O_8$ composition ($x = 0.0$) fired at 300, 600, 800, 1000 and 1200 °C obtained in this study. These spectra are compared with the spectrum of the $Ni_2P_2O_7$ compound prepared by our group [3]. The three absorption bands that appear at

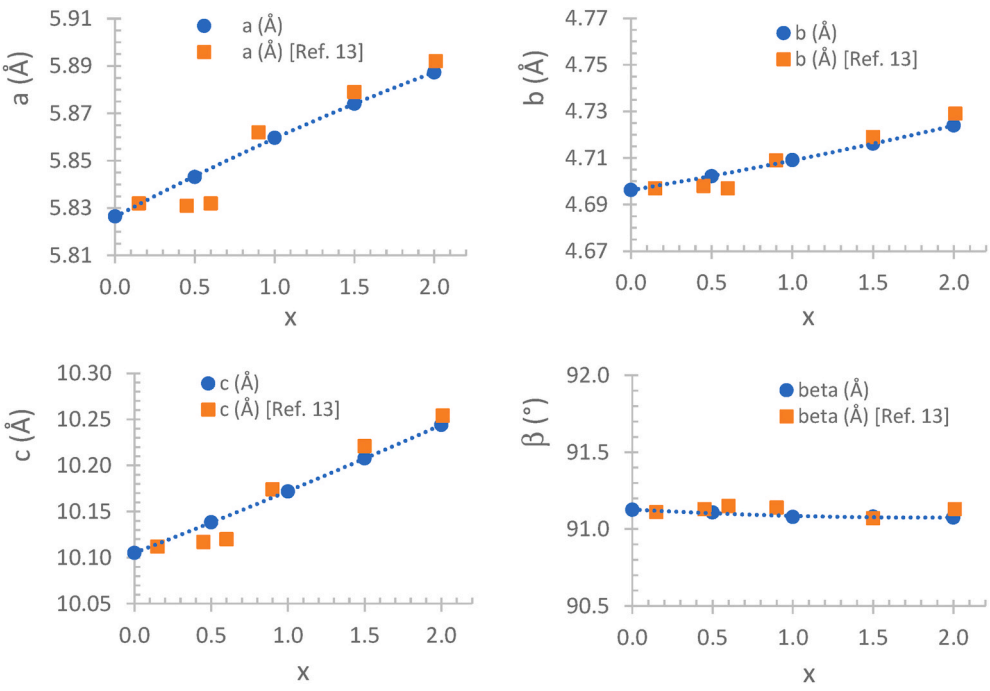

Fig. 4. Unit cell parameters in $Ni_3P_2O_8$ structure from $Co_xNi_{3-x}P_2O_8$ ($0.0 \leq x \leq 2.0$) compositions prepared in this study (●) and values in bibliography [13] (■) at 800 °C.

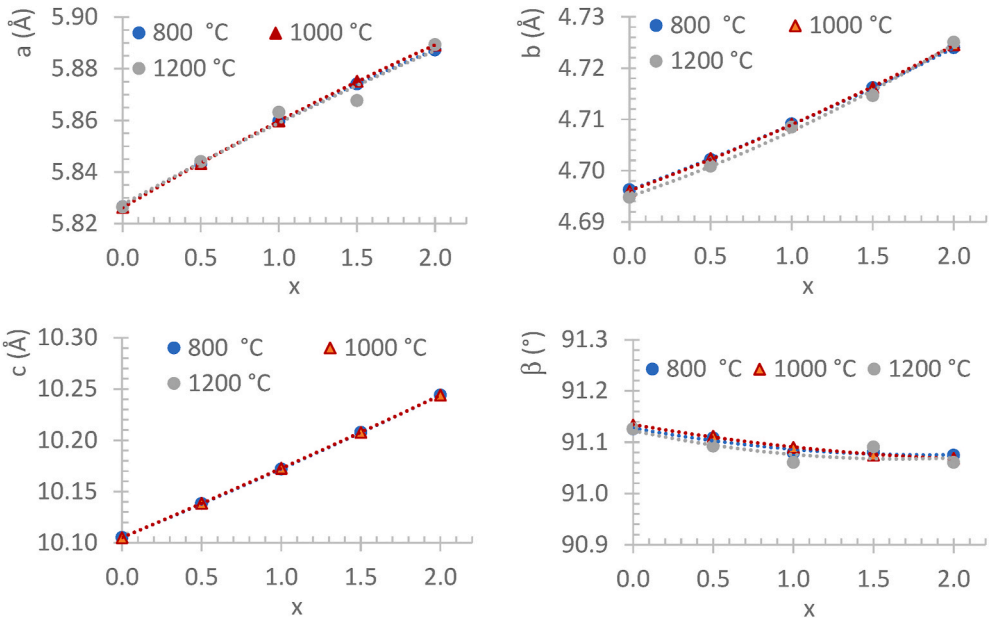

Fig. 5. Unit cell parameters in $Ni_3P_2O_8$ structure from $Co_xNi_{3-x}P_2O_8$ ($0.0 \leq x \leq 2.0$) compositions fired at 800, 1000 and 1200 °C.

1300–1600, 810–830 and 430–490 nm are assigned to Ni^{2+} in an octahedral site. These bands appear at slightly lower wavelength from $Ni_3P_2O_8$ composition (x = 0.0) than from $Ni_2P_2O_7$ composition. In all of the Δ/B, these transitions are: $^3A_2 \rightarrow {}^3T_2(F)$ (first transition), $^3A_2 \rightarrow {}^3T_1(F)$ (second transition) and $^3A_2 \rightarrow {}^3T_1(P)$ (third transition) that generally fall within the ranges 1400–800, 900–500 and 550-370 nm respectively, in octahedral systems [18]. This fact is in accordance with the absence of crossing of the lines that correspond to the variation of the electronic transition energy with Δ/B from a d^8 ion in CN = 6 (Tanabe-Sugano diagram). Changes are due to the higher or the smaller separation of these lines in each Δ/B value. Usually, the absorption band associated with third d-d transition and the charge transfer band of Ni (II)–O appear in the [200−650] wavelength range but they cannot be distinguished. No important changes in the position of the bands are detected between the $Ni_3P_2O_8$ compound fired at T ≥ 800 °C. Bands appear at a wavelength slightly smaller in $Ni_3P_2O_8$ compound than in α-$Ni_2P_2O_7$ compound. Bond strength in the octahedral Ni(II) are similar in $Ni_3P_2O_8$ structure and α-$Ni_2P_2O_7$ structure, with the nephelauxetic ratio β = B'/B approximately 0.70 (where B' is the B Racah parameter experimental obtained from the spectra for spin allowed bands, and B is the B Racah parameter for the free Ni(II) ion). Average Ni–O distances in octahedral site approximately 2.07–2.08 Å from both $Ni_3P_2O_8$ and α-$Ni_2P_2O_7$ structures indicate a similar covalence in Ni–O bonds of these structures. This is in accordance with the similar melting point in

Table 3
Variation of M − O (M = Co, Ni) distances with composition, structure and temperature from $Co_xNi_{3-x}P_2O_8$ ($0.0 \leq x \leq 3.0$) compositions.

x	Structure		M_o–O 800 °C	M_o–O 1000 °C	M_o–O 1200 °C		M_b-O 800 °C	M_b-O 1000 °C	M_b-O 1200 °C
0.0	$Ni_3P_2O_8$	Ni1–O1(x2)	2.088(2)	2.089(2)	2.088(2)	Ni2–O1	2.083(2)	2.081(2)	2.079(2)
		Ni1–O2(x2)	2.077(2)	2.076(2)	2.075(2)	Ni2–O2	2.035(2)	2.035(2)	2.035(2)
		Ni1–O4(x2)	2.071(2)	2.071(2)	2.070(2)	Ni2–O3	2.106(2)	2.105(2)	2.106(2)
						Ni2–O3	1.993(2)	1.992(2)	1.994(2)
						Ni2–O4	2.186(2)	2.186(2)	2.184(2)
						Ni2–O4	2.084(2)	2.085(2)	2.082(2)
0.5	$Ni_3P_2O_8$	M1-O1(x2)	2.086(2)	2.092(2)	2.092(2)	M2-O1	2.078(2)	2.084(2)	2.083(2)
		M1-O2(x2)	2.083(2)	2.079(2)	2.078(2)	M2-O2	2.036(2)	2.038(2)	2.038(2)
		M1-O4(x2)	2.076(2)	2.077(2)	2.076(2)	M2-O3	2.119(2)	2.112(2)	2.111(2)
						M2-O3	1.996(2)	1.998(2)	1.998(2)
						M2-O4	2.192(2)	2.191(2)	2.190(2)
						M2-O4	2.091(2)	2.092(2)	2.091(2)
1.0	$Ni_3P_2O_8$	M1-O1(x2)	2.086(2)	2.092(2)	2.092(2)	M2-O1	2.077(2)	2.080(2)	2.081(2)
		M1-O2(x2)	2.074(2)	2.075(2)	2.075(2)	M2-O2	2.039(2)	2.041(2)	2.042(2)
		M1-O4(x2)	2.077(2)	2.078(2)	2.078(2)	M2-O3	2.122(2)	2.115(2)	2.114(2)
						M2-O3	2.003(2)	2.005(2)	2.006(2)
						M2-O4	2.198(2)	2.194(2)	2.194(2)
						M2-O4	2.096(2)	2.096(2)	2.096(2)
1.5	$Ni_3P_2O_8$	M1-O1(x2)	2.091(2)	2.093(2)	2.090(2)	M2-O1	2.085(2)	2.085(2)	2.082(2)
		M1-O2(x2)	2.084(2)	2.084(2)	2.082(2)	M2-O2	2.043(2)	2.045(2)	2.042(2)
		M1-O4(x2)	2.087(2)	2.086(2)	2.081(2)	M2-O3	2.120(2)	2.117(2)	2.116(2)
						M2-O3	2.008(2)	2.010(2)	2.010(2)
						M2-O4	2.195(2)	2.195(2)	2.190(2)
						M2-O4	2.103(2)	2.102(2)	2.097(2)
2.0	$Ni_3P_2O_8$	M1-O1(x2)	2.095(2)	2.098(2)	2.098(2)	M2-O1	2.093(2)	2.090(2)	2.089(2)
		M1-O2(x2)	2.090(2)	2.090(2)	2.089(2)	M2-O2	2.053(2)	2.054(2)	2.054(2)
		M1-O4(x2)	2.086(2)	2.087(2)	2.087(2)	M2-O3	2.130(2)	2.127(2)	2.125(2)
						M2-O3	2.018(2)	2.021(2)	2.021(2)
						M2-O4	2.205(2)	2.202(2)	2.201(2)
						M2-O4	2.110(2)	2.109(2)	2.109(2)
2.5	$Co_3P_2O_8$[a]	M2-O1(x2)	1.964(2)	2.018(2)	–	M1-O1	2.276(2)	2.201(2)	–
		M2-O2(x2)	2.120(2)	2.135(2)		M1-O2	2.009(2)	1.954(2)	
		M2-O3(x2)	2.152(2)	2.140(2)		M1-O3	2.041(2)	2.069(2)	
						M1-O4	2.010(2)	2.041(2)	
						M1-O4	1.980(2)	1.993(2)	
3.0	$Co_3P_2O_8$[a]	Co2–O1(x2)	1.876(2)	2.079(2)	–	Co1–O1	2.162(2)	2.266(2)	–
		Co2–O2(x2)	2.133(2)	2.157(2)		Co1–O2	1.908(2)	1.964(2)	
		Co2–O3(x2)	2.222(2)	2.114(2)		Co1–O3	2.023(2)	2.077(2)	
						Co1–O4	1.866(2)	2.009(2)	
						Co1–O4	2.031(2)	2.020(2)	

M_o is M in an octahedral site (the less distorted in $Ni_3P_2O_8$ structure).
M_b is M in the most distorted octahedron in $Ni_3P_2O_8$ structure or M pentacoordinated in the stable $Co_3P_2O_8$ structure.
[a] Stable $Co_3P_2O_8$.

$Ni_3P_2O_8$ compound (1350 °C) than in the $Ni_2P_2O_7$ compound (1395 °C).

From Fig. 7, a higher absorbance is observed approximately 1575 nm in $Ni_2P_2O_7$ fired at 1000 °C or approximately 1800 nm in $Ni_2P_2O_7$ fired at 1200 °C than in $Ni_3P_2O_8$ structure (Ni(II) only in octahedral site). In the α-$Ni_2P_2O_7$ structure, only the half of the Ni(II) ions are in octahedral coordination and the other half of the Ni(II) ions are pentacoordinated. This absorbance approximately 1600–1800 nm is related with the pentacoordinated Ni(II) ion in the α-$Ni_2P_2O_7$ structure [3]. Because the octahedra around Ni2 are more distorted than the octahedra around Ni1 in the $Ni_3P_2O_8$ structure, a shoulder approximately 1730–1780 nm can be detected in the first transition (maximum at 1310–1330 nm) at $T \geq 800$ °C.

Fig. 8 shows the UV–vis–NIR spectra of the $Co_3P_2O_8$ composition ($x = 3.0$) fired at 300, 600, 800 and 1000 °C obtained in this study. These spectra are compared with the spectrum of the $Co_2P_2O_7$ compound prepared by our group [3]. The three absorption bands from a d^7 ion in an octahedral site appear in a different order depending of the Δ/B value. This is because of the lines corresponding to the variation with Δ/B of the energy of the $^4T_1(F) \rightarrow {}^4A_2(F)$ and $^4T_1(F) \rightarrow {}^4T_1(P)$ electronic transitions intersect about Δ/B = 15 (Tanabe-Sugano diagram). So, these transitions are as follows: $^4T_1 \rightarrow {}^4T_2$ (first transition), $^4T_1 \rightarrow {}^4A_2$ (second transition) and $^4T_1 \rightarrow {}^4T_1(P)$ (third transition) when $0 \leq \Delta/B \leq 13$, and $^4T_1 \rightarrow {}^4T_2$ (first transition), $^4T_1 \rightarrow {}^4T_1(P)$ (second transition) and $^4T_1 \rightarrow {}^4A_2$ (third transition) when $\Delta/B \geq 13$. The three bands at 1100, 590 and 498 nm from the $Co_3P_2O_8$ fired composition are assigned to Co (II) in octahedral site with $\Delta/B < 13$. The band at 1100 nm can be assigned to the $^4T_1 \rightarrow {}^4T_2(F)$ transition. The weaker band at 590 nm to the $^4T_1 \rightarrow {}^4A_2(F)$ transition and the multiple structured band at 498 nm to $^4T_1 \rightarrow {}^4T_1(P)$ [18]. The bands assigned to octahedral Co(II) in α-$Co_2P_2O_7$ structure are observed at 1225, 593 and 530 nm [3]. The bands from the first and second transitions appear at closer wavelengths in the $Co_3P_2O_8$ composition than in the $Co_2P_2O_7$ composition. The band assigned to the first transition of the Co(II) ions in the octahedral site ($^4T_1 \rightarrow {}^4T_2(F)$ transition) appear at smaller wavelengths (higher energy) in the $Co_3P_2O_8$ composition with the stable $Co_3P_2O_8$ structure than in the $Co_2P_2O_7$ compound with the α-$Co_2P_2O_7$ structure. The octahedral crystal field (Δ) is slightly higher in $Co_3P_2O_8$ compound than in the $Co_2P_2O_7$ compound. The Co–O bonds in the octahedral sites have a slightly higher covalence in $Co_3P_2O_8$ than in $Co_2P_2O_7$ compounds. Their nephelauxetic ratios, $\beta = B'/B$, are 0.95 and 0.99, respectively (where B' is the B Racah parameter experimental obtained from the spectra for spin allowed bands, and B is the B Racah parameter for the free Co(II) ion). This slightly higher covalence might be related to the smaller average Co–O distance in the octahedral site obtained from the stable $Co_3P_2O_8$ structure (approximately 2.08 Å) than from the α-$Co_2P_2O_7$ structure (2.11 Å [3]) at 800 °C. This result is in accordance with the smaller melting point in $Co_3P_2O_8$ compound (1160 °C) than in the $Co_2P_2O_7$ compound (1240 °C).

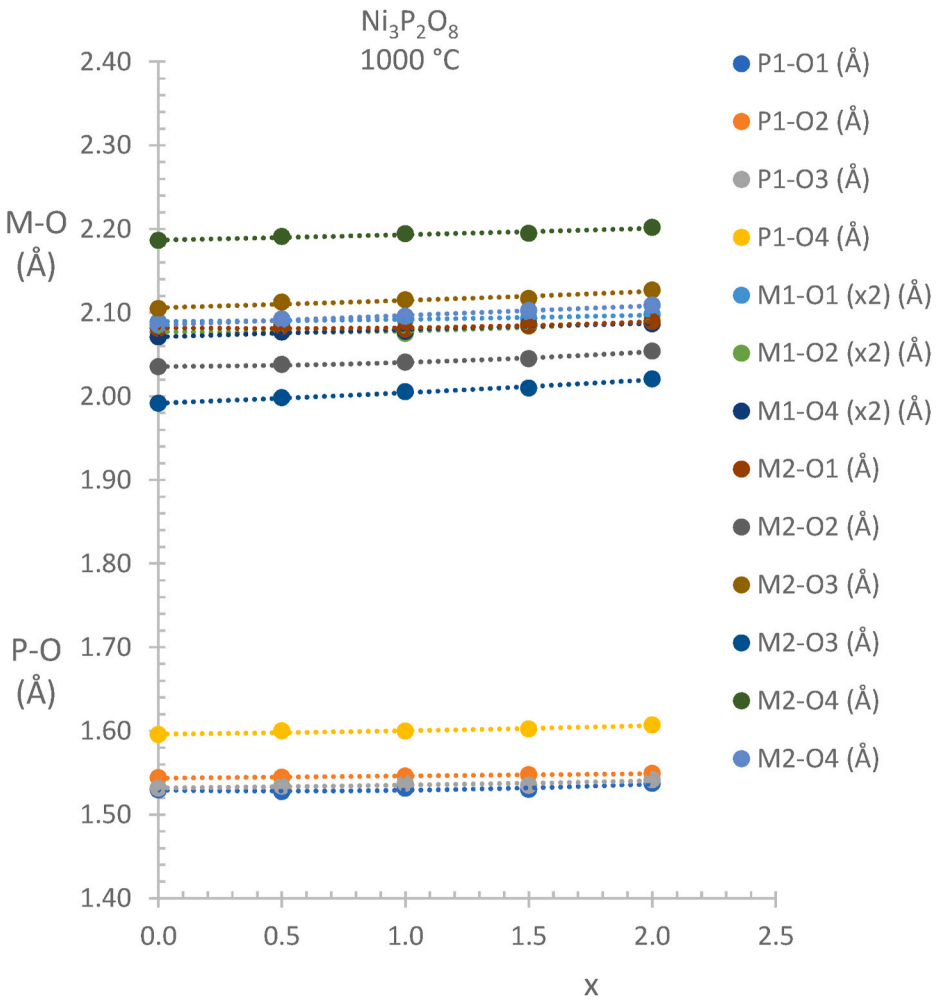

Fig. 6. M − O (M = Co, Ni) and P–O distances in $Co_xNi_{3-x}P_2O_8$ ($0.0 \leq x \leq 2.0$) solid solutions with $Ni_3P_2O_8$ structure at 1000 °C.

Table 4
Variation of P–O distances (M = Co, Ni) distances with composition and temperature in $Ni_3P_2O_8$ (olivine-related $Co_3P_2O_8$) and stable $Co_3P_2O_8$ structures from $Co_xNi_{3-x}P_2O_8$ ($0.0 \leq x \leq 2.0$) compositions.

x	Structure		800 °C	1000 °C	1200 °C
0.0	$Ni_3P_2O_8$	P1–O1	1.529(2)	1.529(2)	1.527(2)
		P1–O2	1.544(2)	1.544(2)	1.544(2)
		P1–O3	1.532(2)	1.531(2)	1.534(2)
		P1–O4	1.595(2)	1.595(2)	1.595/2)
0.5	$Ni_3P_2O_8$	P1–O1	1.530(2)	1.527(2)	1.528(2)
		P1–O2	1.546(2)	1.545(2)	1.545(2)
		P1–O3	1.533(2)	1.534(2)	1.533(2)
		P1–O4	1.599(2)	1.600(2)	1.599(2)
1.0	$Ni_3P_2O_8$	P1–O1	1.529(2)	1.531(2)	1.532(2)
		P1–O2	1.544(2)	1.546(2)	1.546(2)
		P1–O3	1.539(2)	1.537/2)	1.536(2)
		P1–O4	1.603(2)	1.600(2)	1.600(2)
1.5	$Ni_3P_2O_8$	P1–O1	1.525(2)	1.530(2)	1.529(2)
		P1–O2	1.547(2)	1.548(2)	1.546(2)
		P1–O3	1.538(2)	1.535(2)	1.536(2)
		P1–O4	1.604(2)	1.602(2)	1.600(2)
2.0	$Ni_3P_2O_8$	P1–O1	1.535(2)	1.537(2)	1.537(2)
		P1–O2	1.548(2)	1.549(2)	1.549(2)
		P1–O3	1.545(2)	1.542(2)	1.541(2)
		P1–O4	1.609(2)	1.607(2)	1.606(2)
2.5	$Co_3P_2O_8$	P1–O1	1.601(2)	1.564(2)	–
		P1–O2	1.542(2)	1.569(2)	
		P1–O3	1.526(2)	1.524(2)	
		P1–O4	1.572(2)	1.541(2)	
3.0	$Co_3P_2O_8$	P1–O1	1.617(2)	1.549(2)	–
		P1–O2	1.713(2)	1.547(2)	
		P1–O3	1.515(2)	1.537(2)	
		P1–O4	1.505(2)	1.569(2)	

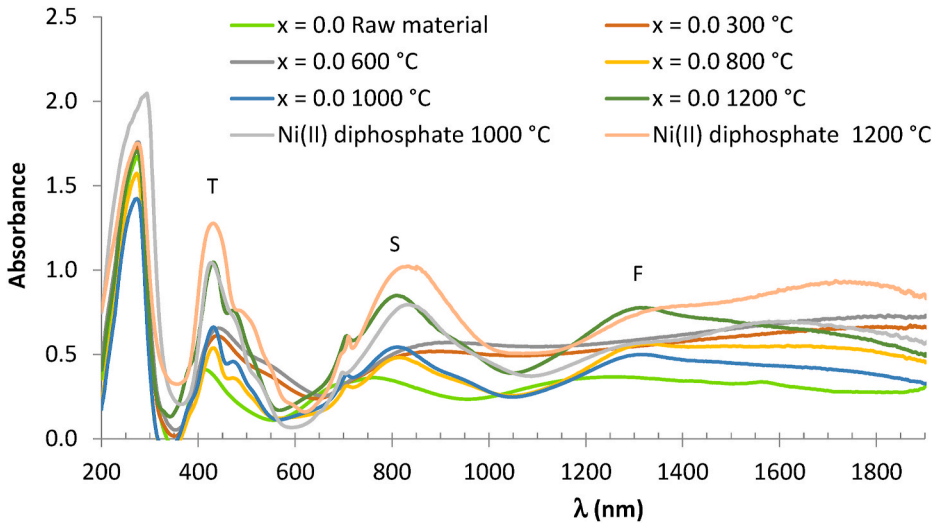

Fig. 7. UV–vis–NIR spectra of $Ni_3P_2O_8$ (x = 0.0) fired at 300, 600, 800, 1000 and 1200 °C and $Ni_2P_2O_7$ compound fired at 1000 and 1200 °C. Ni(II) CN = 6: (F) $^3A_2 \rightarrow {}^3T_2(F)$, (S) $^3A_2 \rightarrow {}^3T_1(F)$, (T) $^3A_2 \rightarrow {}^3T_1(P)$.

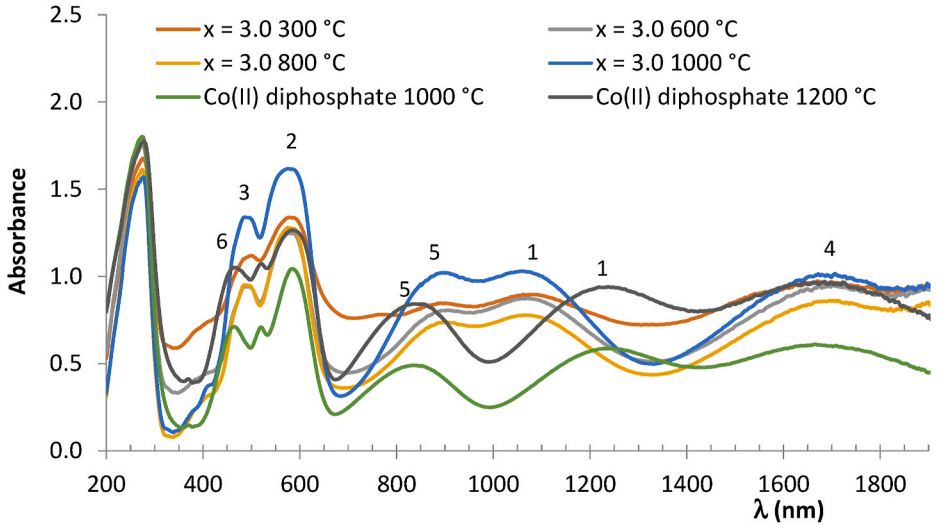

Fig. 8. UV–vis–NIR spectra of $Co_3P_2O_8$ (x = 3.0) fired at 300, 600, 800 and 1000 °C and $Co_2P_2O_7$ compound fired at 1000 and 1200 °C. Co(II) CN = 6: (1) $^4T_1 \rightarrow {}^4T_2$, (2) $^4T_1 \rightarrow {}^4A_2$, (3) $^4T_1 \rightarrow {}^4T_1(P)$. Co(II) CN = 5: (4) $^4A_2 \rightarrow {}^4A_1$, (5) $^4A_2 \rightarrow {}^4E$, (6) $^4A_2 \rightarrow {}^4E(P)$.

Bands at 1707, 904 and 498 nm (Fig. 8) are assigned to Co(II) in a square-planar pyramid coordination ($^4A_2 \rightarrow {}^4A_1(F)$, $^4A_2 \rightarrow {}^4E(F)$ and $^4A_2 \rightarrow {}^4E(P)$ transitions) according to the stable $Co_3P_2O_8$ phase detected by XRD. These bands appear at 1689, 850 and 474 nm in the $Co_2P_2O_7$ compound with α-$Co_2P_2O_7$ structure [3].

Fig. 9 shows the UV–vis–NIR spectra of $Co_xNi_{3-x}P_2O_8$ ($0.0 \leq x \leq 3.0$) solid solutions at 800, 1000 and 1200 °C. Changes in the shape and the position bands is in accordance with the crystalline phase developed in each composition. Between 800 and 1200 °C, $Co_xNi_{3-x}P_2O_8$ solid solutions with $Ni_3P_2O_8$ structure (or olivine-related $Co_3P_2O_8$ structure) are obtained when $x \leq 2.0$ and with the stable when $x \geq 2.5$. From $x \leq 2.0$ compositions, spectra are similar to $Ni_3P_2O_8$ spectrum (x = 0.0) with the increase in absorbance in 450–650 nm when Co(II) amount increases. Bands assigned to Ni^{2+} in the octahedral site appear at 1366-1290 nm (first transition), 794 nm (second transition) and 448 nm (third transition). Bands assigned to Co^{2+} in an octahedral site appear at 1366-1290 nm (first transition), 560–599 nm (second transition) and 470–540 nm (third transition). So, the observed colour of these materials have a mixture of yellow (first transition of the octahedral Ni(II) ion), violet (second transition of the octahedral Co(II) ion) and orange-red (third transition of the octahedral Co(II) ion). These results are in accordance with the octahedral coordination of all of the Co(II) ions in the developed olivine-related $Co_3P_2O_8$ structure (isostructural with the $Ni_3P_2O_8$ structure) when $x \leq 2.0$ at 800 and 1000 °C and when $x < 2.0$ at 1200 °C. The spectra obtained from $x \geq 2.5$ compositions are similar to spectrum of $Co_3P_2O_8$ with the stable structure (x = 3.0) at temperatures from 800 to 1000 °C. No significant changes in spectra were detected when minor crystalline phases are detected together with the main crystalline phase. The small amount of phase with the stable $Co_3P_2O_8$ structure (approximately 13% when x = 2.0) or with the $Ni_3P_2O_8$ structure (approximately 5% when x = 2.5) does not change the spectrum shape significantly. According with the strength of the Co–O bonds, the band assigned to the first transition of the Co(II) ions in the octahedral site ($^4T_1 \rightarrow {}^4T_2$ transition) appears at smaller wavelengths in solid solutions with the stable $Co_3P_2O_8$ structure than in solid solutions with the $Ni_3P_2O_8$ structure. The position of the band assigned to Co(II) in a square-planar pyramid coordination ($^4A_2 \rightarrow {}^4E$ transition) in solid solutions with the stable $Co_3P_2O_8$ structure appears at slightly higher wavelength than the second transition of the Ni(II) ion: $^3A_2 \rightarrow {}^3T_1(F)$). The bands corresponding to the second and third electronic transitions

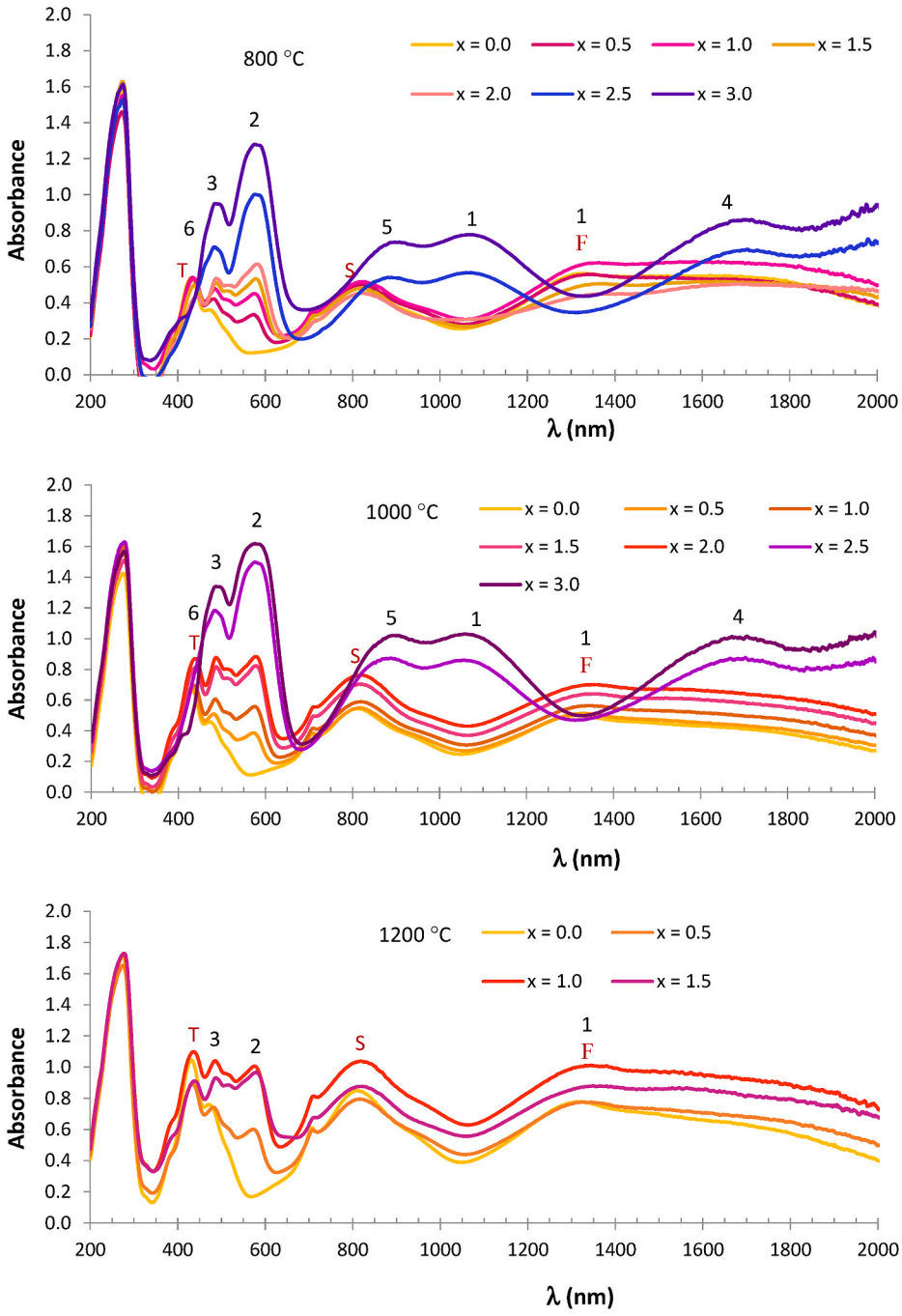

Fig. 9. UV–vis–NIR spectra of $Co_xNi_{3-x}P_2O_8$ ($0.0 \leq x \leq 3.0$) compositions fired at 800, 1000 and 1200 °C. Ni(II) CN = 6: (F) $^3A_2 \rightarrow {}^3T_2$, (S) $^3A_2 \rightarrow {}^3T_1$, (T) $^3A_2 \rightarrow {}^3T_1$(P). Co(II) CN = 6: (1) $^4T_1 \rightarrow {}^4T_2$, (2) $^4T_1 \rightarrow {}^4A_2$, (3) $^4T_1 \rightarrow {}^4T_1$(P). Co(II) CN = 5: (4) $^4A_2 \rightarrow {}^4A_1$, (5) $^4A_2 \rightarrow {}^4E$, (6) $^4A_2 \rightarrow {}^4E$(P).

of the octahedral Co(II) ion overlap with distinguishable maximums at 590 and 498 nm. The higher absorbance between 457 and 628 nm in these spectra make the observable colour of these materials red-violet-blue with an important blue amount (maximum absorbance at 590 nm) when $x \geq 2.5$.

Fig. 10 compares spectra in compositions with Co:Ni ratio 1:1 with orthophosphate ($Co_{1.5}Ni_{1.5}P_2O_8$) and diphosphate ($CoNiP_2O_7$) structures. At 1000 °C, $CoNiP_2O_7$ composition is green [3] (L* = 54.06, a* = −0.74, b* = +12.42) and $Co_{1.5}Ni_{1.5}P_2O_8$ composition is reddish pink (L* = 58.93, a* +23.51, b* = +10.77, Table 5). The position of the third transition band of the Ni(II) ion: $^3A_2 \rightarrow {}^3T_1$(P) can be related with the yellow amount (positive b* value). In composition with diphosphate structure the $^4A_2 \rightarrow {}^4E$(P) transition band from Co(II) ion with CN = 5 also contributes at this band. The blue amount (negative b*) can be related with the second transition band of the octahedral Co(II) ion: $^4T_1 \rightarrow {}^4A_2$. So, the similar absorbance of these bands explains the green observed colour in $CoNiP_2O_7$ composition. The position of the third transition band of the octahedral Co(II) ion: $^4T_1 \rightarrow {}^4T_1$(P) can be related with the variation of the red amount (positive a*). The higher value in the red amount is due to the higher absorbance in 490–550 nm in the orthophosphate structure than in the diphosphate structure. At 1200 °C, the colour of the $Co_{1.5}Ni_{1.5}P_2O_8$ composition is dark pink (L* = 48.44, a* +14.98, b* = +4.68) with a red amount (a*) higher than $CoNiP_2O_7$ composition at the same temperature (reddish brown colour; L* = 41.05, a* = +3.99, b* = +11.64 [3]). Although similar absorbance in the 490–550 nm range is obtained in $Co_{1.5}Ni_{1.5}P_2O_8$ and $CoNiP_2O_7$

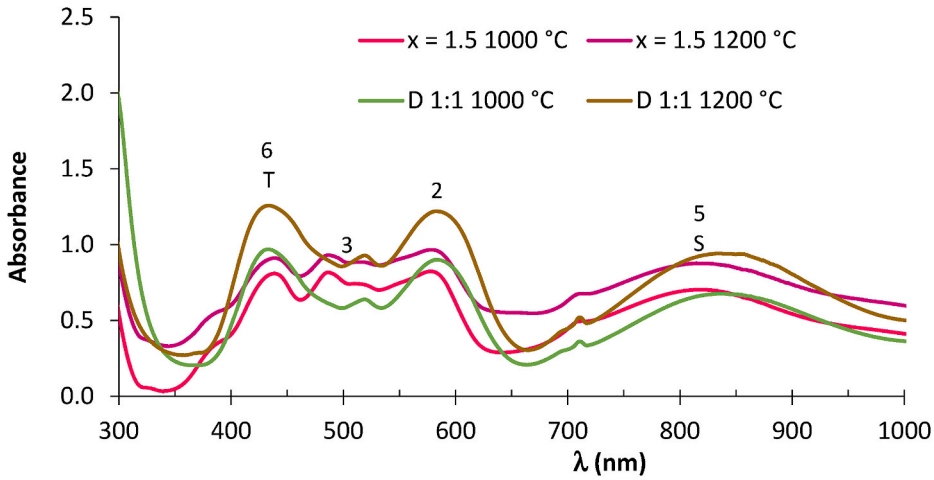

Fig. 10. UV–vis–NIR spectra of $Co_{1.5}Ni_{1.5}P_2O_8$ (x = 1.5) and $CoNiP_2O_7$ (D 1:1) compositions fired at 1000 and 1200 °C. Ni(II) CN = 6: (S) $^3A_2 \rightarrow {}^3T_1$, (T) $^3A_2 \rightarrow {}^3T_1$(P). Co(II) CN = 6: (2) $^4T_1 \rightarrow {}^4A_2$, (3) $^4T_1 \rightarrow {}^4T_1$(P). Co(II) CN = 5: (5) $^4A_2 \rightarrow {}^4E$, (6) $^4A_2 \rightarrow {}^4E$(P).

Table 5
CIE L* a* b* colour parameters and observed colour in $Co_xNi_{3-x}P_2O_8$ ($0.0 \leq x \leq 3.0$) compositions.

x		65 °C	300 °C	600 °C	800 °C	1000 °C	1200 °C
0.0	L*	86.76	77.05	78.98	86.18	86.28	79.53
	a*	- 5.80	+9.85	+11.95	+3.46	+3.09	+4.76
	b*	+18.34	+22.70	+23.53	+30.41	+37.66	+52.43
	Colour	Pale green	Beige	Beige	Yellow	Yellow	Yellow
0.5	L*	67.56	65.47	61.23	80.06	76.42	64.56
	a*	- 4.05	+2.41	+2.59	+9.80	+12.21	+15.02
	b*	- 7.31	+5.49	+5.53	+20.05	+24.00	+24.04
	Colour	Pale blue	Dark grey	Grey	Beige	Beige	Beige
1.0	L*	56.51	53.16	47.78	71.50	69.12	48.62
	a*	+0.86	+1.13	+0.96	+12.52	+16.72	+20.35
	b*	−6.37	- 1.24	- 2.16	+12.66	+16.47	+14.84
	colour	Grey	Dark grey	Dark grey	Beige	Pink	Red
1.5	L*	43.48	52.52	55.15	70.46	58.93	48.44
	a*	+13.74	+0.59	+1.35	+15.14	+23.51	+14.98
	b*	+2.77	- 7.55	- 6.42	+6.23	+10.77	+4.68
	colour	Reddish	Dark grey	Lilac	Pink	Reddish pink	Dark pink
2.0	L*	51.59	51.08	52.85	66.21	57.11	45.33
	a*	+17.02	+0.61	+2.80	+15.40	+23.84	+6.26
	b*	+4.15	- 12.68	- 12.75	- 1.80	+1.60	−9.62
	colour	Pink	Violet	Violet	Lilac	Reddish pink	Violet
2.5	L*	60.04	45.50	41.06	52.76	36.24	–
	a*	+20.74	+2.62	+6.64	+17.25	+24.09	–
	b*	+1.62	- 10.76	−13.64	- 15.72	- 11.02	–
	colour	Pink	Purple	Purple	Violet	Purple	
3.0	L*	34.71	44.46	41.50	41.68	32.12	–
	a*	+9.30	+4.97	+13.38	+18.35	+25.99	–
	b*	−38.52	- 10.27	- 21.88	- 25.99	- 25.56	–
	colour	Purple	Purple	Purple	Purple	Purple	

At 1200 °C, $Ni_2P_2O_7$: L* = 71.39, a* = +17.54, b* = +55.52; $Co_2P_2O_7$: L* = 34.84, a* = +11.53, b* = −11.41 [3].

compositions while in the $Co_{1.5}Ni_{1.5}P_2O_8$ composition is the maximum absorbance in spectrum, in the $CoNiP_2O_7$ composition the third transition band of the Ni(II) ion and the second transition band of the octahedral Co(II) ion are present with higher absorbance.

Table 5 shows the CIE L* a* b* colour parameters and observed colour in $Co_xNi_{3-x}P_2O_8$ ($0.0 \leq x \leq 3.0$) compositions dried at 65 °C and fired at 300, 600, 800, 1000 and 1200 °C. At 800 and 1000 °C, yellow, beige or pink materials are obtained when $x \leq 1.5$ and lilac, violet and purple materials when $x \geq 2.0$. At this temperature, $Ni_3P_2O_8$ solid solutions are detected when $x \leq 1.5$ or 2.0. The incorporation of Co(II) in the $Ni_3P_2O_8$ structure decreases the yellow amount (the positive b* value decreases) and increases the red amount (increases the positive a* value). The incorporation of Ni(II) in solid solutions with the stable $Co_3P_2O_8$ structure when $x \geq 2.0$ decreases the blue amount (negative b* value) and the variation of the red amount (a*) is small in these compositions. Fig. 11 shows the variation of the a* and b* parameters with composition from the $Co_xNi_{3-x}P_2O_8$ ($0.0 \leq x \leq 3.0$) compositions fired at 1000 and 1200 °C. At 1200 °C, the yellow amount decreases with x and the red amount increases until x = 1.0 and then decreases from a* = 20.35 in x = 1.0 to a* = 6.26 in x = 2.0.

The optimal composition to obtain materials with red colouration can be established when x = 1.0, $CoNi_2P_2O_8$ composition with the highest a* value (a* = 20.25) at 1200 °C. It is comparable with the red material obtained from the $Mg_{0.5}Cu_{1.5}V_{1.8}P_{0.2}O_7$ composition fired at 600 °C (a* = 22.61), but this colouration is not stable with the temperature (a* = + 0.80 at 1200 °C) [19]. The a* value is smaller (dark orange, L * = 51.35, a* = 15.94, b* = 17.57) from the doping of Pr^{4+} or Tb^{4+} in $La_2Ce_2O_7$ with disordered defect fluorite type structure at 900 °C for 10 h [20]. At 1200 °C, when $0.0 \leq x \leq 1.5$, $Co_xNi_{3-x}P_2O_8$ solid solutions with the $Ni_3P_2O_8$ structure are stable and might be used as

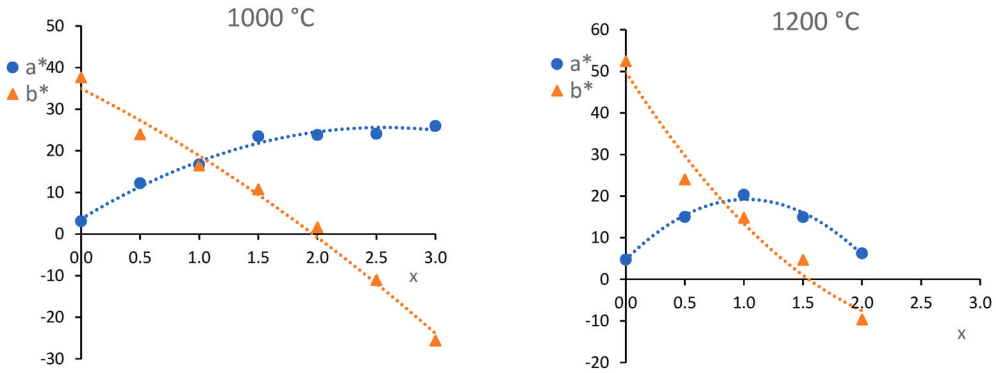

Fig. 11. CIE a* b* colour parameters in $Co_xNi_{3-x}P_2O_8$ $0.0 \leq x \leq 3.0$ compositions fired at 1000 and 1200 °C. (For interpretation of the references to colour in this figure legend, the reader is referred to the Web version of this article.)

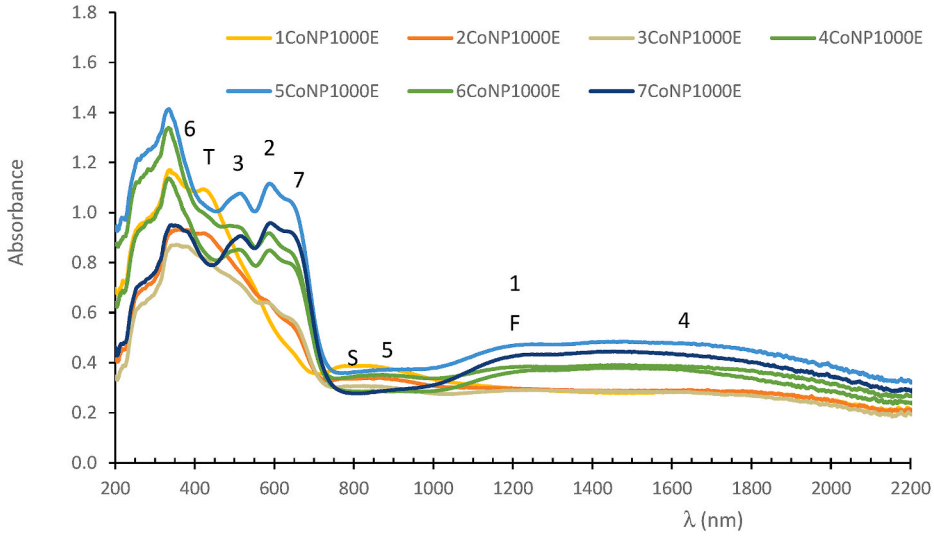

Fig. 12. UV–vis–NIR spectra of 4% of $Co_xNi_{3-x}P_2O_8$ $(0.0 \leq x \leq 3.0)$ compositions fired at 1000 °C. Ni(II) CN = 6: (F) $^3A_2 \rightarrow {}^3T_2$, (S) $^3A_2 \rightarrow {}^3T_1$, (T) $^3A_2 \rightarrow {}^3T_1$(P). Co (II) CN = 6: (1) $^4T_1 \rightarrow {}^4T_2$, (2) $^4T_1 \rightarrow {}^4A_2$, (3) $^4T_1 \rightarrow {}^4T_1$(P). Co(II) CN = 5: (4) $^4A_2 \rightarrow {}^4A_1$, (5) $^4A_2 \rightarrow {}^4E$, (6) $^4A_2 \rightarrow {}^4E$(P). Co(II) CN = 4 (tetrahedral coordination): (7) $^4A_2 \rightarrow {}^4T_1$(P).

Table 6
CIE L* a* b* colour parameters from glazed tiles obtained from $Co_xNi_{3-x}P_2O_8$ $(0.0 \leq x \leq 3.0)$ materials fired at 1000 °C.

x	L*	a*	b*	Observed colour
0.0	56.01	+17.03	+33.72	Yellowish beige
0.5	53.43	+10.06	+21.07	Brown
1.0	52.93	+6.57	+14.22	Greenish brown
1.5	44.99	+3.92	+8.50	Green
2.0	32.85	+0.48	−1.37	Blue
3.0	43.10	+0.07	- 2.75	Blue

yellow, beige, red or dark pink paint pigments.

The pinhole defect is not detected in the enamelling of samples. They are avoided in phosphates. Loss of oxygen is not obtained under the conditions of preparation of the materials because the Co_3O_4 compound is not obtained. Cobalt violet phosphate, $Co_3P_2O_8$, is included in the DCMA Classification of the Mixed Metal Oxide Inorganic Coloured Pigments (DCMA-8-11-1) [21], but $Ni_3P_2O_8$ is not included in this classification. Fig. 12 shows the visible spectra in glazed tiles prepared with 4% $Co_xNi_{3-x}P_2O_8$ $(0.0 \leq x \leq 3.0)$ materials fired at 1000 °C. The absorbance at 490–550 nm (responsible of red observed colour) is present when $x > 1.0$. A new band at 650 is observed in the enamelled samples in all samples containing cobalt ($x > 0.0$). This band can be assigned to tetrahedral Co(II) ion, $^4A_2 \rightarrow {}^4T_1$(P) and is responsible for the colour change of the samples. When $x > 1.0$, the blue amount is higher in enamelling samples than in powder samples at the same temperature. In the conditions of this study and with the commercial glaze used, the colour parameters (L* a* b*) of enamelled samples are different from those obtained for powder samples. Yellowish brown, brown, green and blue colourings are obtained in the different compositions (Table 6). Because of their stability at the working temperature in the ceramic industry, $Co_xNi_{3-x}P_2O_8$ $(0.0 \leq x \leq 1.5)$ solid solutions with the $Ni_3P_2O_8$ structure may be used as yellowish brown, brown, green and blue ceramic pigments.

4. Conclusions

$Co_xNi_{3-x}P_2O_8$ $(0.0 \leq x \leq 3.0)$ compositions synthesized via the chemical co-precipitation method are not crystalline or poorly crystalline at 600 °C. At 800 °C, the $Ni_3P_2O_8$ structure is developed when $0.1 \leq x \leq 0.2$ and the stable $Co_3P_2O_8$ structure when $x \geq 2.5$. They are the only crystalline phase at 1000 °C. At 1200 °C, the crystalline $Ni_3P_2O_8$ phase is detected in compositions with $0.0 \leq x \leq 2.0$; although, the crystalline stable $Co_3P_2O_8$ phase also appears when $1.5 \leq x \leq 2.0$. Compositions with $x > 2.0$ melted at this temperature.

Increasing the unit cell parameters with x is consistent with the replacement of the Ni(II) ion by the larger Co(II) ion in the $Ni_3P_2O_8$

structure when solid solutions are formed ($0.0 \leq x \leq 2.0$). At 800, 1000 and 1200 °C, similar values of unit cell parameters were obtained in $Ni_3P_2O_8$ structure and at 800–1000 °C in the stable $Co_3P_2O_8$ structure ($2.5 \leq x \leq 3.0$). These solid solutions are stable at these temperatures. From $Co_xNi_{3-x}P_2O_8$ ($0.0 \leq x \leq 2.0$) solid solutions with the $Ni_3P_2O_8$ structure, no significant distortions are detected.

The shape and position of the bands in UV-V spectra are in accordance with the crystalline phase developed in each composition. From $x \leq 2.0$ compositions, spectra are similar to $Ni_3P_2O_8$ spectrum with the increase in absorbance in 450–650 nm when Co(II) amount increases. Bands are assigned to Ni(II) and Co(II) in the octahedral site. Yellow, beige, pink and red materials are obtained when $x \leq 1.5$. The incorporation of Co(II) in the $Ni_3P_2O_8$ structure decreases the yellow amount and increases the red amount. The $CoNi_2P_2O_8$ composition ($x = 1.0$) with the highest a* value ($a^* = 20.25$) at 1200 °C can be established as the optimal composition to obtain materials with red colouration.

Lilac, violet and purple materials are obtained when $x \geq 2.0$. The incorporation of Ni(II) in solid solutions with the stable $Co_3P_2O_8$ structure decreases the blue amount. In these compositions, the red amount is high (a* approximately 24–26) at 1000 °C, but it decreases with x at 1200 °C.

From glazed tiles prepared with 4% $Co_xNi_{3-x}P_2O_8$ ($0.0 = x \leq 3.0$) materials fired at 1000 °C, yellowish brown, brown, green and blue colourations are obtained. Because of their temperature stability, these materials may be used as ceramic pigments to avoid the loss of oxygen obtained with the use of Co(II) oxides.

Declaration of competing interest

The authors declare that they have no known competing financial interests or personal relationships that could have appeared to influence the work reported in this paper.

The authors declare that they have no conflict of interest.

Acknowledgements

We gratefully acknowledge the financial support provided by Spain's Ministerio de Ciencia, Innovación y Universidades, project MAT2016-78155-C2-1-R.

References

[1] Development of asymmetric device using $Co_3(PO_4)_2$ as a positive electrode for energy storage application, J. Mater. Sci. Mater. Electron. 30 (2019) 7435–7446, https://doi.org/10.1007/s10854-019-01057-x.

[2] A. El Jazouli, B. Tbib, A. Demourgues, M. Gaudon, Structure and Colour of diphosphate pigments with square pyramid environment around chromophore ions (Co^{2+}, Ni^{2+}, Cu^{2+}), Dyes Pigments 104 (2014) 67–74.

[3] M.A. Tena, R. Mendoza, C. Trobajo, J.R. García, S. García-Granda, $Co_2P_2O_7$–$Ni_2P_2O_7$ solid solutions: structural characterization and color, 00, J. Am. Ceram. Soc. (2018) 1–10, https://doi.org/10.1111/jace.16158.

[4] M.A. Tena, Rafael Mendoza, José R. García, Santiago García-Granda, "Structural characterization and colour of $Ni_3V_xP_{2-x}O_8$ ($0 \leq x \leq 2$) and $Ni_2V_yP_{2-y}O_7$ ($0 \leq y \leq 2$) materials", Results in Physics 7 (2017) 1095–1105, https://doi.org/10.1016/j.rinp.2017.02.021.

[5] M.A. Tena, Characterization of $Mg_xM_{2-x}P_2O_7$ (M = Cu and Ni) solid solutions, J. Eur. Ceram. Soc. 32 (2012) 389–397, https://doi.org/10.1016/j.jeurceramsoc.2011.09.018.

[6] C. Calvo, R. Faggiani, Structure of nickel orthophosphate, Can. J. Chem. 53 (1975) 1516–1520.

[7] Inorganic Crystal Structure Database (ICSD Web). Fachinformationszentrum (FIZ, Karlsruhe, Germany).

[8] G. Berthet, J.C. Joubert, E.F. Bertaut, Vacancies ordering in new metastable orthophosphates $[Co_3]P_2O_8$ and $[Mg_3]P_2O_8$ with olivine-related structure, Z. Kristallogr. 136 (1972) 98–105.

[9] G. Anders, Nord, theodor stefanidis, structure refinements of Co3(PO4)2. A note on the reliability of powder diffraction studies, Acta Chem. Scand. A37 (1983) 715–721.

[10] H.M. Rietveld, A profile refinement method for nuclear and magnetic structures, J. Appl. Crystallogr. 2 (1969) 65–71.

[11] Rodriguez-Carvajal J (September 2018-ILL-JRC), Fullprof.2k Computer ProgRam, version 6.50, France.

[12] L. Chapon, Rutherford Appleton Laboratory, UK) and Rodriguez-Carvajal J, FPStudio Computer Program, Institut Laue Langevin, France, August 2008. version 2.0.

[13] G. Anders, Nord, Crystallographic studies of olivine-related sarcopside-type solid solutions, Z. für Kristallogr. - Cryst. Mater. 166 (1984) 159–176, https://doi.org/10.1524/zkri.1984.166.3-4.159.

[14] Y. Tang, Z. Liu, W. Guo, T. Chen, Y. Qiao, S. Mu, Y. Zhao, F. Gao, Honeycomb-like mesoporous cobalt nickel phosphate nanospheres as novel materials for high performance supercapacitor, Electrochim. Acta 190 (2016) 118–125.

[15] Baskar Senthilkuma, Ahamed Irshad, Prabeer Barpanda, Cobalt and nickel phosphates as multifunctional air-cathodes for rechargeable hybrid sodium-air battery applications, ACS Appl. Mater. Interfaces 11 (2019) 33811–33818 (Supporting Information).

[16] Jingchao Zhang, Yong Yang, Zhicheng Zhang, Xiaobin Xu, Xun Wang, Rapid synthesis of mesoporous $Ni_xCo_{3x}(PO_4)_2$ hollow shells showing enhanced electrocatalytic and supercapacitor performance, J. Mater. Chem. 2 (2014) 20182.

[17] Commission Internationale del'Eclairage, Recommendations on Uniform Color Spaces, Color Difference Equations, Phychometrics Color Terms, Bureau Central de la CIE, Paris, 1971. Supplement no. 2 of CIE Publication No. 15 (E1-1.31).

[18] A.B.P. Lever, Inorganic Electronic Spectroscopy, second ed., Elsevier Science B. V., The Netherlands, 1977, pp. 507–511.

[19] M.A. Tena, Rafael Mendoza, David Martinez, Camino Trobajo, José R. García, Santiago García-Granda, Characterization of yellow and red inorganic pigments from $Mg_{0.5}Cu_{1.5}V_xP_{2-x}O_7$ ($0 \leq x \leq 2$) solid solutions, SN Appl. Sci. 2 (1106) (2020) 1–10, https://doi.org/10.1007/s42452-020-2917-7.

[20] B. Huang, Y. Xiao, C. Huang, J. Chen, X. Sun, Environment-friendly pigments based on praseodymium and terbium doped La2Ce2O7 with high near-infrared reflectance: synthesis and characterization, Dyes Pigments 147 (2017) 225–233.

[21] DCMA classification and chemical description of the mixed metal oxide inorganic coloured pigments, in: Metal Oxides and Ceramics Colors Subcommittee, Dry Color Manufacturer's Ass. Washington DC, second ed., 1982.